Resource

Cell Reports

Post-translational Regulation of Cas9 during G1 Enhances Homology-Directed Repair

Graphical Abstract

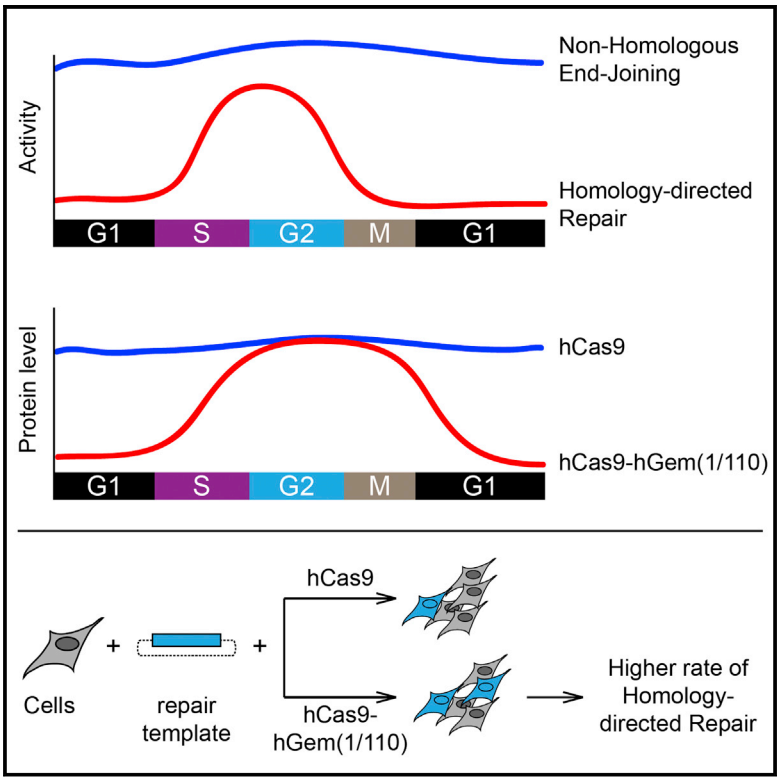

Authors

Tony Gutschner, Monika Haemmerle, Giannicola Genovese, Giulio F. Draetta, Lynda Chin

Correspondence

tgutschner@mdanderson.org (T.G.), lchin@mdanderson.org (L.C.)

In Brief

Using a protein engineering approach, Gutschner et al. generate a Cas9 fusion protein to control genome editing in time and space. Coupling Cas9 protein levels to cell-cycle dynamics results in higher site-specific integration events.

Highlights

- Homology-directed repair (HDR) enables generation of site-specific Knockins
- HDR is restricted to S/G2 and competes with non-homologous end-joining repair
- Cas9-hGem(1/110), a cell-cycle-tailored genome-editing tool, is generated
- Cas9-hGem(1/110) increases the rate of HDR up to 1.87-fold compared to wild-type Cas9

Gutschner et al., 2016, Cell Reports *14*, 1555–1566
February 16, 2016
http://dx.doi.org/10.1016/j.celrep.2016.01.019

CellPress

Cell Reports
Resource

Post-translational Regulation of Cas9 during G1 Enhances Homology-Directed Repair

Tony Gutschner,[1,*] Monika Haemmerle,[2,3] Giannicola Genovese,[1] Giulio F. Draetta,[1,4,5] and Lynda Chin[1,4,*]
[1]Department of Genomic Medicine, The University of Texas MD Anderson Cancer Center, Houston, TX 77030, USA
[2]Department of Gynecologic Oncology and Reproductive Medicine, The University of Texas MD Anderson Cancer Center, Houston, TX 77030, USA
[3]Institute of Pathology, University Hospital Heidelberg, 69120 Heidelberg, Germany
[4]Institute for Applied Cancer Science, The University of Texas MD Anderson Cancer Center, Houston, TX 77030, USA
[5]Department of Molecular and Cellular Oncology, The University of Texas MD Anderson Cancer Center, Houston, TX 77030, USA
*Correspondence: tgutschner@mdanderson.org (T.G.), lchin@mdanderson.org (L.C.)
http://dx.doi.org/10.1016/j.celrep.2016.01.019

SUMMARY

CRISPR/Cas9 induces DNA double-strand breaks that are repaired by cell-autonomous repair pathways, namely, non-homologous end-joining (NHEJ), or homology-directed repair (HDR). While HDR is absent in G1, NHEJ is active throughout the cell cycle and, thus, is largely favored over HDR. We devised a strategy to increase HDR by directly synchronizing the expression of Cas9 with cell-cycle progression. Fusion of Cas9 to the N-terminal region of human Geminin converted this gene-editing protein into a substrate for the E3 ubiquitin ligase complex APC/Cdh1, resulting in a cell-cycle-tailored expression with low levels in G1 but high expression in S/G2/M. Importantly, Cas9-hGem(1/110) increased the rate of HDR by up to 87% compared to wild-type Cas9. Future developments may enable high-resolution expression of genome engineering proteins, which might increase HDR rates further, and may contribute to a better understanding of DNA repair pathways due to spatiotemporal control of DNA damage induction.

INTRODUCTION

The ability to modify the genetic information of an organism enables one to study the function of its genes, e.g., during normal development. Moreover, genome editing holds the promise to model and reverse disease-causing variants on the cellular and organismal level. However, until recently, easy-to-use, flexible, and efficient genome-editing tools were missing. The discovery of the RNA-guided endonuclease Cas9 from the type II CRISPR (clustered regularly interspaced palindromic repeats) system revolutionized the field of genome engineering. Initially, CRISPRs had been discovered in bacteria and archaea (Ishino et al., 1987; Mojica et al., 2000) and were later shown to be derived from plasmid and viral origins (Bolotin et al., 2005; Mojica et al., 2005; Pourcel et al., 2005). The CRISPR-Cas system was finally characterized as an adaptive defense system targeting foreign nucleic acids (Barrangou et al., 2007; Brouns et al., 2008; Marraffini and Sontheimer, 2008). The three known CRISPR-Cas systems use different mechanisms to achieve nucleic acid recognition and cleavage (Makarova et al., 2011a, 2011b). While type I and type III systems use large multiprotein complexes, the type II system requires only a single protein, Cas9, to achieve RNA-guided DNA recognition and cleavage (Gasiunas et al., 2012; Hale et al., 2009; Haurwitz et al., 2010; Jinek et al., 2012). Cas9 is a large multifunctional protein with two nuclease domains, HNH and RuvC-like, acting together to introduce DNA double-strand breaks (DSBs) into invading plasmids and phages (Bolotin et al., 2005; Garneau et al., 2010; Haft et al., 2005; Makarova et al., 2006). The *S. pyogenes* CRISPR-Cas9 protein depends on a tracrRNA (*trans*-activating crRNA [CRISPR RNA]) and requires the formation of a tracrRNA:crRNA duplex to direct DNA cleavage (Deltcheva et al., 2011; Jinek et al., 2012). In 2013, the CRISPR-Cas9 system was put into the spotlight of genome engineering: three studies used humanized versions of *S. pyogenes* and *S. thermophiles* Cas9, together with either custom-designed single-guide RNAs (sgRNAs) or tracrRNA co-expressed with custom-designed crRNAs, to edit the genome of human and murine cells (Cong et al., 2013; Jinek et al., 2013; Mali et al., 2013b). Since then, Cas9-mediated genome editing has been applied to various mammalian cell systems and diverse model organisms (Doudna and Charpentier, 2014; Hsu et al., 2014; Mali et al., 2013a; Sander and Joung, 2014).

Once recruited to its target sequence in eukaryotes, Cas9 induces a DNA DSB, which is repaired either by the non-homologous end-joining pathway (NHEJ) or by homology-directed repair (HDR). While the NHEJ pathway is important for the creation of loss-of-function alleles due to the generation of variable insertions and deletions (indels), the HDR pathway enables precise repair or site-specific integration of exogenous DNA sequences into the genome. The ability of Cas9 to introduce DSBs at defined, customizable positions has made it possible to reproduce tumor-associated alterations in cellulo and in living animals (Choi and Meyerson, 2014; Maddalo et al., 2014; Platt et al., 2014; Sánchez-Rivera et al., 2014; Xue et al., 2014) and to correct disease-causing mutations in adult stem cells (Schwank et al., 2013). Moreover, genome-wide sgRNA libraries have been developed

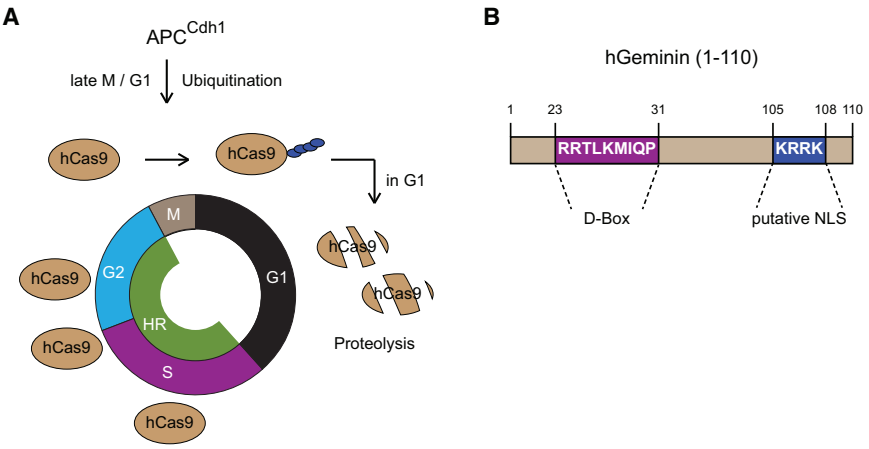

C

...CCCCCGAGGATAATGAGCAGAAACAGCTGTTTGTGGAACAGCACAAGCACTACCTGGACG
AGATCATCGAGCAGATCAGCGAGTTCTCCAAGAGAGTGATCCTGGCCGACGCTAATCTGGAC
AAAGTGCTGTCCGCCTACAACAAGCACCGGGATAAGCCCATCAGAGAGCAGGCCGAGAATAT
CATCCACCTGTTTACCCTGACCAATCTGGGAGCCCCTGCCGCCTTCAAGTACTTTGACACCA
CCATCGACCGGAAGAGGTACACCAGCACCAAAGAGGTGCTGGACGCCACCCTGATCCACCA
GAGCATCACCGGCCTGTACGAGACACGGATCGACCTGTCTCAGCTGGGAGGCGACAAAAGG
CCGGCGGCCACGAAAAAGGCCGGCCAGGCAAAAAAGAAAAAG***GGATCC***(BamHI)***AAGCTT***
(HindIII)ATGAATCCCAGTATGAAGCAGAAACAAGAAGAAATCAAAGAGAATATAAAGAATAGTTC
TGTCCCAAGAAGAACTCTGAAGATGATTCAGCCTTCTGCATCTGGATCTCTTGTTGGAAGAGA
AAATGAGCTGTCCGCAGGCTTGTCCAAAAGGAAACATCGGAATGACCACTTAACATCTACAAC
TTCCAGCCCTGGGGTTATTGTCCCAGAATCTAGTGAAAATAAAAATCTTGGAGGAGTCACCCA
GGAGTCATTTGATCTTATGATTAAAGAAAATCCATCCTCTCAGTATTGGAAGGAAGTGGCAGAA
AAACGGAGAAAGGCGCTG**TAA*CTCGAG***(XhoI)***GAATTC***(EcoRI)

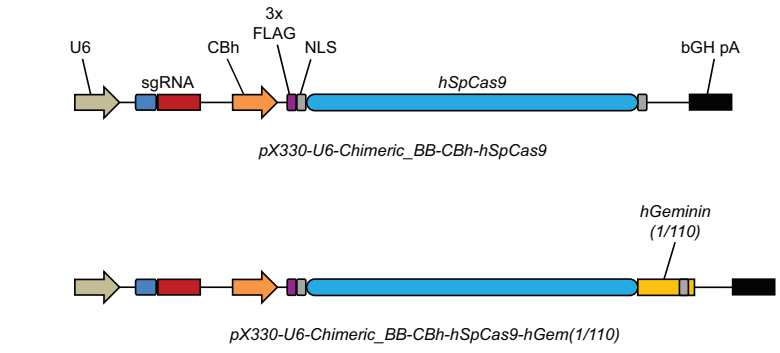

Figure 1. Conversion of hCas9 into an APC/Cdh1 Substrate

(A) HR activity is restricted to the S phase and G2 phase of the cell cycle. Thus, hCas9-induced DNA DSBs in the G1 phase will likely be repaired via NHEJ, which reduces the chance for HDR to occur in subsequent cell-cycle phases. Importantly, the activity of the APC/Cdh1 E3 ubiquitin ligase complex is high in the late M and G1 phases, allowing proteolysis of substrates. Hence, converting hCas9 into an APC/Cdh1 substrate would limit genome-editing activity to the S/G2/M phases and might increase chances for HDR to occur.

(B) Schematic overview of the N-terminal region of human Geminin. The D-Box motif mediates recognition by the anaphase-promoting complex and subsequent proteolysis in the G1 phase of the cell cycle.

(C) Nucleotide sequence of the C-terminal part of the hCas9-hGem(1/110) fusion construct. The humanized Cas9 sequence (black) is followed by the first 330 nt of the open reading frame of human Geminin (red) and a stop codon (TAA).

(D) Schematic overview of expression vectors used throughout this study. NLS, nuclear localization signal; CBh, hybrid chicken beta actin promoter.

to perform pooled loss-of-function screens (Wang et al., 2014; Zhou et al., 2014) and to identify essential genes (Shalem et al., 2014; Wang et al., 2015). The latter approaches, thereby, rely on the error-prone NHEJ pathway to identify critical genes and potential drug targets. However, functional analysis of disease-associated sequence variants requires a precise site-specific knockin, which is a more challenging task due to the rather low overall activity of the HDR pathway. Importantly, the activity of the HDR pathway is restricted to the late S and G2 phases of the cell cycle, while the NHEJ pathway dominates DNA repair during the G1, S, and G2 phases (Heyer et al., 2010). Thus, the error-prone NHEJ pathway out-competes the HDR pathway, which reduces the likelihood for precise insertions, deletions, or base substitutions at the DSB. Chemical or genetic interruptions of the NHEJ pathway can favor HDR, but these can be difficult to achieve or might be harmful to cells (Shrivastav et al., 2008; Vasquez et al., 2001). Here, we introduce a strategy to increase the rate of HDR by controlling the expression and, thus, the activity of the CRISPR-Cas9 endonuclease in a temporal manner.

RESULTS

Recently, the Doudna lab has shown that the controlled delivery of pre-assembled Cas9 ribonucleoprotein (RNP) complexes into chemically synchronized cells results in robust HDR-mediated genome editing (Lin et al., 2014). However, this approach requires the optimization of cell-cycle synchronization protocols for individual cell types and involves multiple in vitro steps for the synthesis, purification, and assembly of sgRNA-Cas9 RNP complexes.

A complementary yet unexplored strategy to control Cas9 activity in a cell-cycle-dependent temporal manner is to convert it into a substrate of the APC/Cdh1 complex, the major cell-cycle-controlling E3 ubiquitin ligase. The APC/Cdh1 complex is active in the late M and G1 phases and promotes the ubiquitination of a variety of proteins, which leads to their degradation (Figure 1A). One direct target of the APC/Cdh1 complex is the replication licensing factor Geminin, which contains a destruction box motif in its N-terminal region mediating APC recognition (Figure 1B). In 2008, Sakaue-Sawano et al. showed that the first 110 amino

acids of human Geminin are sufficient to confer nuclear localization and cell-cycle-dependent proteolysis of fluorescent reporter proteins, which allowed the visualization of spatiotemporal dynamics of cell-cycle progression (Sakaue-Sawano et al., 2008). To enable post-translational control over Cas9 in human cells, we sought to engineer a Cas9-Geminin fusion protein, hereinafter referred to as hCas9-hGem(1/110). We envisioned that the fusion of the first 110 amino acids of Geminin with hCas9 would result in a proteolytic destruction of hCas9-hGem(1/110) in the late M and G1 phases, and accumulation of hCas9-hGem(1/110) in the S/G2/M phases, which would directly couple genome editing with HDR activities (Figure 1A). We genetically inserted the first 330 nucleotides of the open reading frame of human Geminin (Figure 1C) into the commonly used, bicistronic pX330-U6-Chimeric_BB-CBh-hSpCas9 vector to generate the pX330-U6-Chimeric_BB-CBh-hSpCas9-hGem(1/110) plasmid (Figure 1D). This allowed a direct side-by-side comparison of both constructs in subsequent protein expression and genome-editing experiments.

hCas9-hGem(1/110) Protein Expression Is Cell Cycle Dependent

First, we wanted to see whether the engineered fusion protein is expressed at the expected size and whether we could detect any difference in the steady-state protein levels of wild-type hCas9 and hCas9-hGem(1/110) in human cell lines. We transfected equal amounts of pX330-hSpCas9 or pX330-hSpCas9-hGem(1/110) plasmids into HEK293T cells and, 72 hr later, performed western blot and real-time qPCR expression analysis. Both hCas9 variants were detected at their expected molecular size (Figure 2). Notably, the hCas9-hGem(1/110) variant showed ~50% reduced steady-state protein expression (Figure 2A), which was not due to reduced mRNA expression (Figure 2B). Cell-cycle analysis of unsynchronized HEK293T cells identified ~42% of cells in the G1 phase and ~58% in the S/G2/M phases (Figure S1A), which is in good agreement with the observed ~50% reduction in hCas9-hGem(1/110) protein levels, indicating a post-translational regulation. Steady-state protein levels of hCas9-hGem(1/110) were also lower in A549 lung cancer cells (Figure 2C), which was, again, not caused by reduced mRNA expression (Figure 2D). This suggests that the post-translational regulation is not cell type restricted.

Next, we speculated that arresting cells in G2/M might increase the protein expression of hCas9-hGem(1/110) with no or only minor effects on wild-type hCas9. Hence, we transfected equal amounts of the respective plasmids and synchronized HEK293T cells with nocodazole. Indeed, hCas9-hGem(1/110) protein levels strongly increased in synchronized cells, reaching wild-type hCas9 levels, and mirrored endogenous Geminin expression (Figure 2E). The same expression pattern was observed in A549 cells (Figure S1B). This is in line with the endogenous activity profile of the APC/Cdh1 complex, suggesting that the post-translational regulation of hCas9-hGem(1/110) is, indeed, directly controlled by the major cell-cycle-controlling E3 ubiquitin ligase.

Finally, to rule out non-specific drug effects on protein expression, we performed live-cell sorting. Transfected, unsynchronized cells were separated according to their DNA content (Figures S1C and S1D) and followed by analysis of protein levels from G0/G1 and S/G2/M sub-populations. Strikingly, hCas9-hGem(1/110), but not wild-type hCas9, showed a cell-cycle-dependent expression that mimicked the oscillating expression pattern of endogenous Geminin (Figure 2F). Hence, hCas9 expression can be controlled in a temporal manner by an endogenous eukaryotic regulatory circuit.

Enhanced Homology-Directed Repair at a Single-Copy Reporter Gene Locus by hCas9-hGem(1/110)

We hypothesized that restricting the expression and activity of hCas9 to the S/G2/M phases of the cell cycle would result in increased HDR-mediated repair of DSBs. To compare the two hCas9 variants in an HDR assay, we took advantage of a cell system similar to one recently established (Mali et al., 2013b). Here, HEK293T cells were engineered to contain a single copy of a disrupted *EGFP* gene (Figure 3A). EGFP expression can be restored by simultaneous delivery of a promoterless *EGFP* repair plasmid, an AAVS1-specific guide RNA (sgAAVS1), and hCas9. HDR-mediated restoration of a functional *EGFP* gene can be followed by flow cytometry analysis. In fact, co-delivery of all three components resulted in a dose-dependent increase in the number of EGFP-positive cells (Figure 3B). This dose dependency might be due to altered molecular ratios between the sgRNA:protein complexes and the repair plasmid. Importantly, hCas9-hGem(1/110) more efficiently stimulated EGFP restoration under all conditions tested, resulting in 1.28- to 1.87-fold higher HDR rates, compared to wild-type hCas9 (Figure 3C). Of note, increasing amounts of hCas9 expression plasmids translated into increasing amounts of hCas9 proteins, with hCas9-hGem(1/110) showing a markedly reduced steady-state expression under all conditions (Figure 3D). Therefore, less hCas9 protein can increase the rate of exogenous donor-template-mediated HDR when expressed at the right time during cell-cycle progression.

hCas9-hGem(1/110) Enhanced HDR at the Endogenous *MALAT1* Non-coding RNA Locus

To compare the rates of HDR at an endogenous locus, we chose to target the long non-coding RNA (lncRNA) *MALAT1* (Gutschner et al., 2013a). Loss-of-function analysis of lncRNAs using traditional genome-editing technology has been challenging, due to the lack of an open reading frame in these transcripts. Consequently, alternative targeting strategies have been developed that rely on HDR-mediated gene disruption or replacement (Haemmerle and Gutschner, 2015). Our previous work identified a region within the *MALAT1* gene locus that is susceptible to site-specific genome editing (Gutschner et al., 2011, 2013b). Thus, we wanted to test whether the engineered hCas9-hGem(1/110) could enhance HDR at this endogenous locus. We used the CRISPR design tool (http://crispr.mit.edu/) to search for sgRNAs targeting the *MALAT1* promoter region (Figure 4A). We identified a suitable and active sgMALAT1 that modified the intended locus in a dose-dependent manner (Figure 4B). Interestingly, reduced hCas9-hGem(1/110) protein levels under these conditions (Figure 4C) provoked similar rates of indel formation, indicating that NHEJ pathway activity is very high throughout the cell cycle in HEK293T cells.

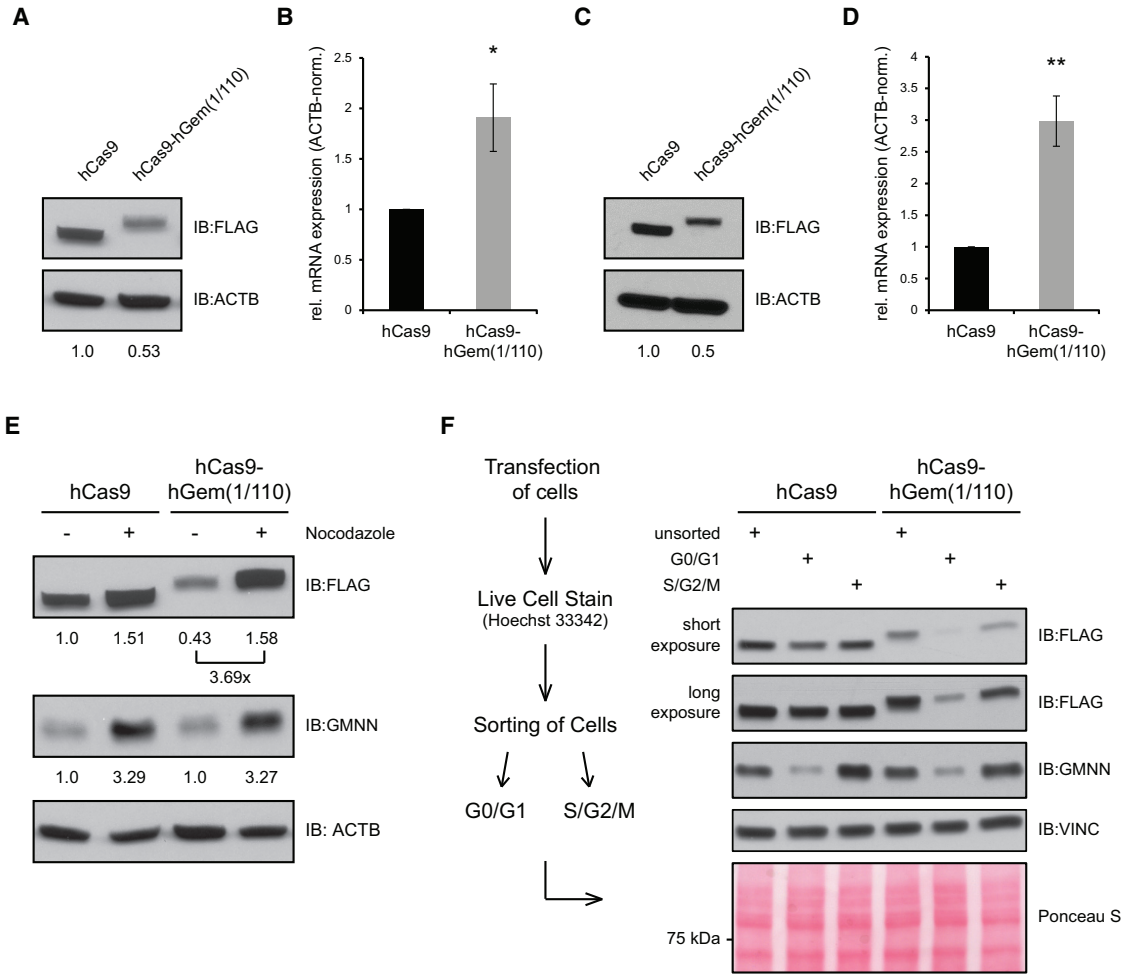

Figure 2. Cell-Cycle-Tailored Expression of hCas9-hGem(1/110)

(A–D) Representative western blots showing steady-state levels of hCas9 and hCas9-hGem(1/110) in HEK293T (A) and A549 (C) cells 72 hr after transfection with 500 ng (HEK293T) or 2 μg (A549) expression vector each. ACTB serves as loading control. (B and D) Real-time qPCR analysis of hCas9 transcript levels in HEK293T (B) and A549 (D) cells 72 hr after transfection. Shown is the mean ± SEM of three independent experiments. IB, immunoblot; rel., relative; norm., normalized. *$p < 0.05$; **$p < 0.01$.

(E) Representative western blot showing expression of hCas9 variants and endogenous Geminin in HEK293T after nocodazole treatment (200 ng/ml; 22 hr).

(F) Representative western blot showing cell-cycle-resolved expression of hCas9 variants and endogenous Geminin in HEK293T. Vinculin and Ponceau S are shown to verify equal protein loading.

All experiments were performed in biological replicates (n = 3). See also Figure S1.

To assess HDR activities at the *MALAT1* locus, we generated a repair donor plasmid that contained a multiple cloning site (MCS) flanked by homology arms (Figure 4D). Co-transfection of this donor plasmid with sgMALAT1-containing pX330-hSpCas9 or pX330-hSpCas9-hGem(1/110) vectors led to successful integration of the MCS sequence, as determined by XhoI-induced cleavage of respective PCR products. Importantly, hCas9-hGem(1/110) was able to induce higher absolute rates of exogenous donor-template-mediated HDR (Figure 4E). On average, hCas9-hGem(1/110) increased the absolute rates of HDR at the *MALAT1* locus from ~9.7% to ~13.8% (hCas9 and hCas9-hGem(1/110), respectively) (Figure 4F), with reduced steady-state protein levels (Figure 4G). This makes hCas9-hGem(1/110) about 1.42-fold more efficient at this particular locus and suggests that it can be a valuable gene-editing tool, especially for genomic loci that are difficult to analyze, such as non-coding regions of the genome.

Transient Cell Cycle Arrest in the G2/M Phases Further Increased HDR

Finally, we wanted to investigate whether it would be possible to further increase rates of HDR at the *MALAT1* locus by transiently arresting cells in the G2/M phases. To test this, we transfected HEK293T cells with sgMALAT1-containing pX330-hSpCas9 or pX330-hSpCas9-hGem(1/110) vectors, together with the MCS-containing repair plasmid (1 μg each) and treated the cells as depicted in Figure 5A. Indeed, we observed a significant enhancement of targeted integration at the *MALAT1* locus after

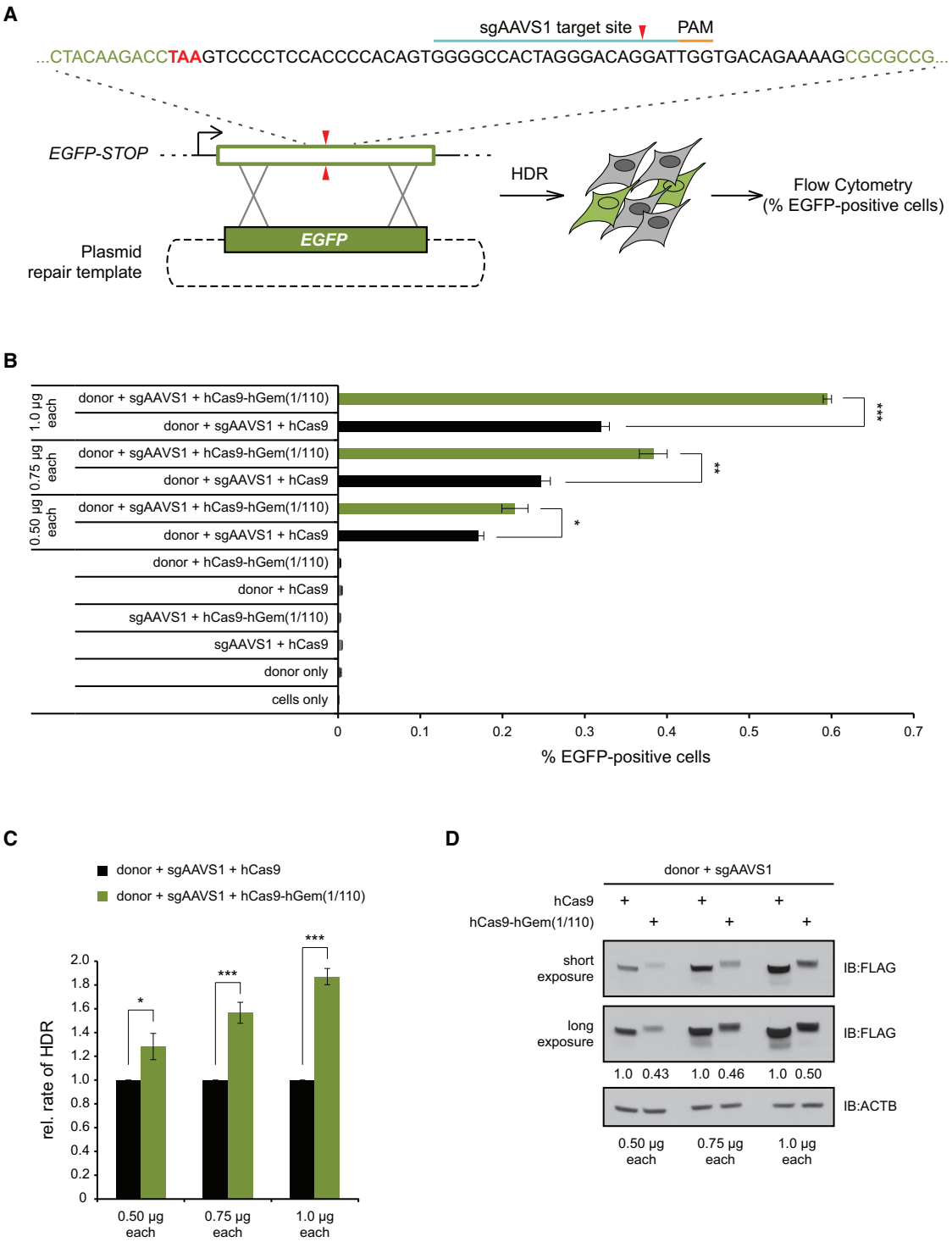

Figure 3. hCas9-hGem(1/110) Enhances HDR at a Monoallelic Reporter Gene Locus

(A) Overview of the engineered single-copy *EGFP* locus in the HEK293T reporter cell line.

(B) Percent EGFP-positive cells analyzed 72 hr after transfection with indicated amounts of pX330 variants and repair plasmid.

(C) Relative (rel.) rates of HDR. Rate of hCas9 set to 1.

(D) Representative western blot showing expression of hCas9 variants in HEK293T 72 hr after transfection with the indicated plasmid amounts. IB, immunoblot.

All experiments were performed in biological replicates ($n \geq 3$). Data indicate the mean ± SEM. *$p < 0.05$; **$p < 0.01$; ***$p < 0.001$.

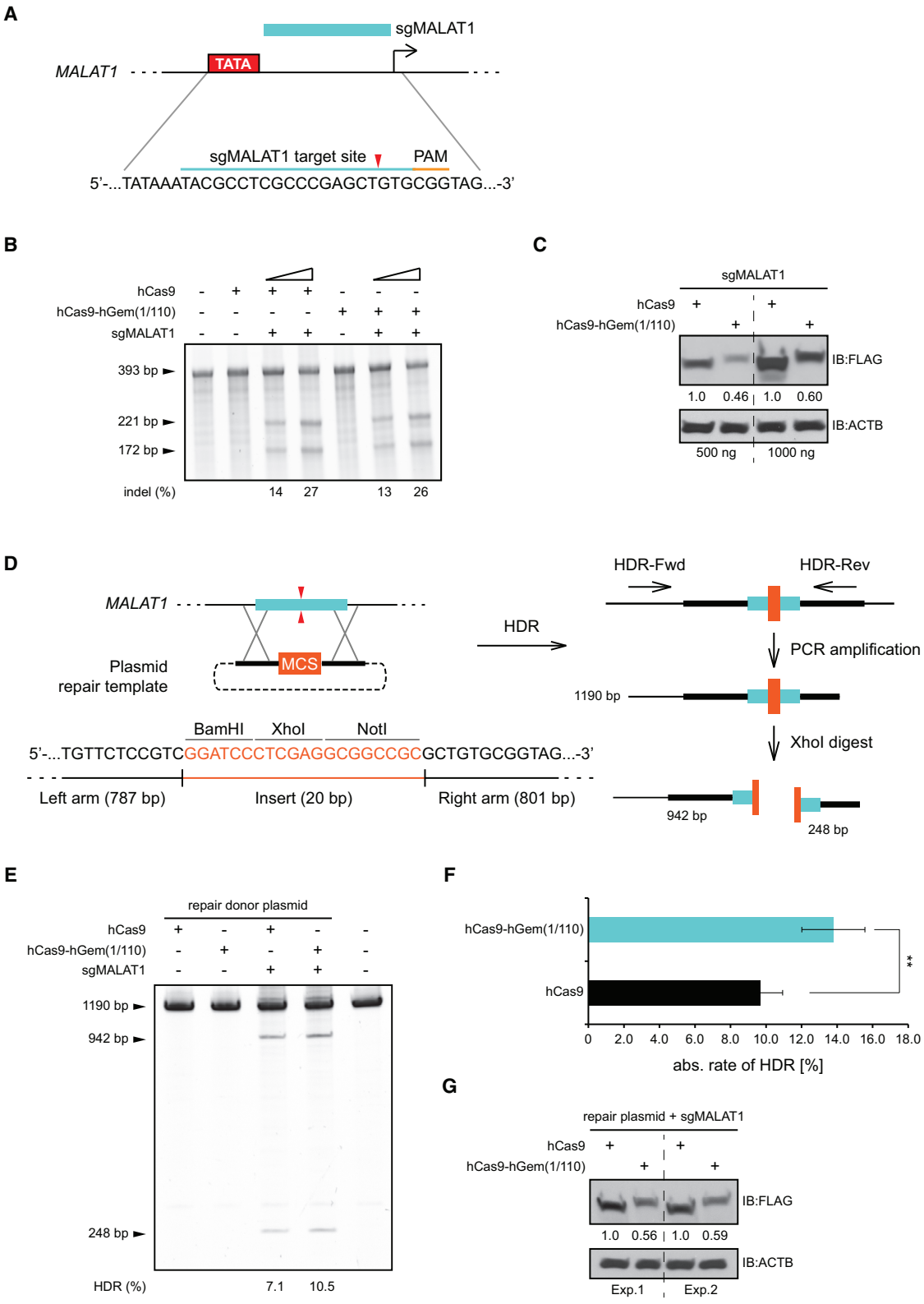

Figure 4. hCas9-hGem(1/110) Enhances Exogenous Donor-Template-Mediated HDR at an Endogenous Non-coding RNA Locus

(A) Schematic overview of the endogenous *MALAT1* non-coding RNA locus. The target region of the designed sgMALAT1 is highlighted (blue line). Cleavage occurs between the TATA box and transcriptional start site (red arrow).

(legend continued on next page)

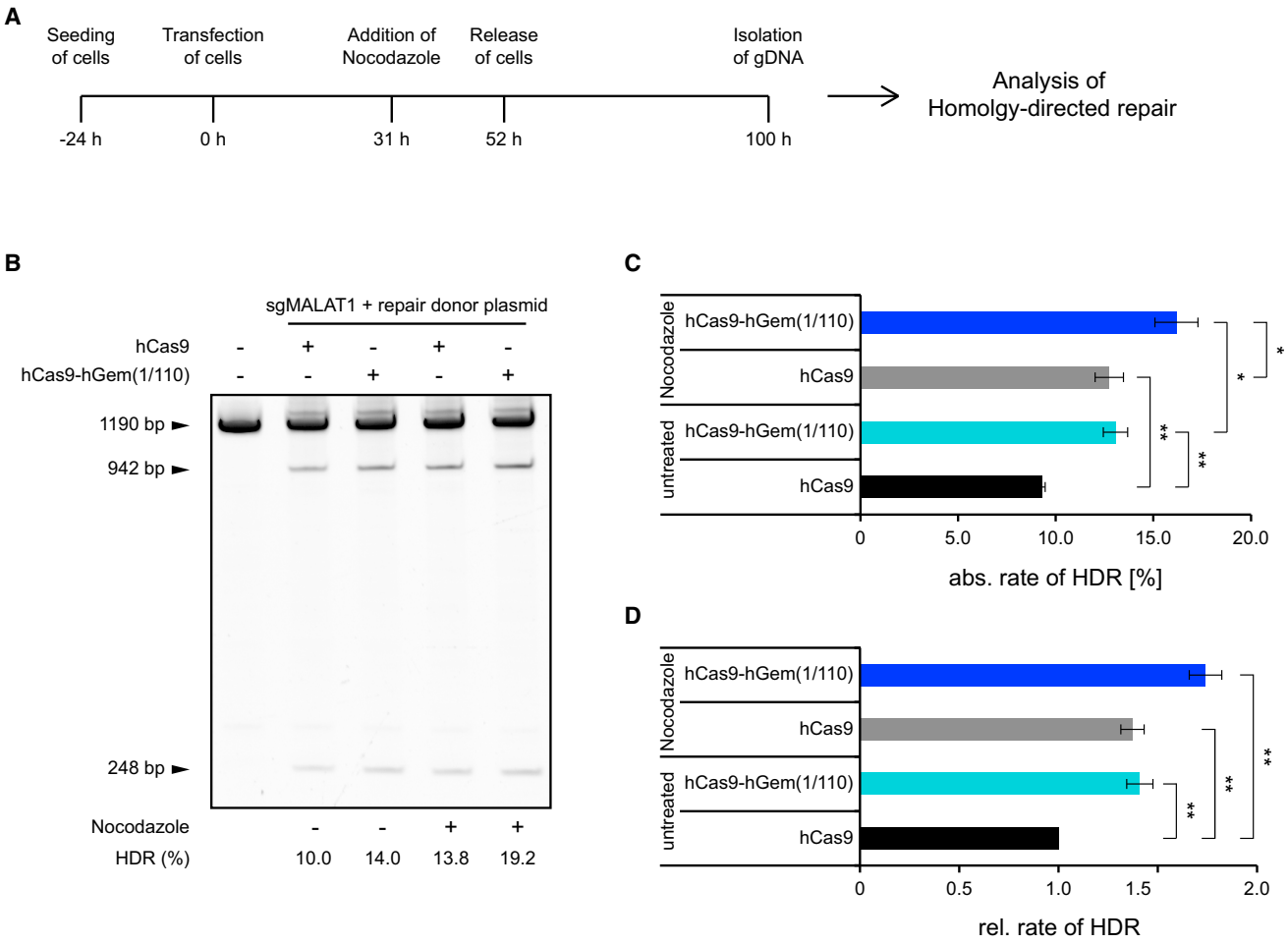

Figure 5. Transient G2/M Cell-Cycle Arrest Further Increases HDR

(A) Timeline of cell treatments. HEK293T cells were transfected with pX330 and repair donor plasmids (1 μg each). Nocodazole (200 ng/ml) was added to transiently arrest cells in the G2/M stahe. After 21 hr, medium was changed, and cells continued proliferation for an additional 48 hr.

(B) HDR frequency in HEK293T cells (with or without nocodazole) analyzed 100 hr after transfection of 1 μg pX330 and 1 μg *MALAT1* repair donor plasmid.

(C and D) Absolute (abs.) percentage (C) and relative (rel.) rate (D) of HDR at the endogenous *MALAT1* locus. Relative rate of hCas9 set to 1. All experiments were performed in biological replicates (n = 4).

Data indicate the mean ± SEM. *p < 0.05; **p < 0.01. See also Figure S2.

a transient nocodazole-induced cell-cycle arrest (Figure 5B). The absolute rate of HDR increased from 9.2% to 13% and from 12.7% to 16.2% for hCas9 and hCas9-hGem(1/110), respectively (Figure 5C). The combined usage of hCas9-hGem(1/110) and nocodazole was ~1.74-fold more efficient than hCas9 alone (Figure 5D). This finding suggests that the combination of hCas9-hGem(1/110) with alternative methods or treatments that enhance HDR activity or transiently prolong the S/G2/M phases might be a valid strategy to achieve efficient site-specific integration of exogenous DNA sequences. In line with this, we tested the impact of SCR7, a recently described DNA Ligase IV inhibitor (Srivastava et al., 2012). SCR7 suppresses the

(B) SURVEYOR assay showing dose-dependent activity of sgMALAT1 in HEK293T cells 72 hr after transfection of pX330 plasmids.

(C) Representative western blot showing differential and dose-dependent expression of hCas9 variants under genome-editing conditions (co-expression of sgMALAT1 from pX330 vectors; 72 hr, n = 2). IB, immunoblot.

(D) Strategy for analyzing hCas9-induced HDR at the endogenous *MALAT1* locus after integration of an MCS (orange). Localization of HDR-PCR primer is highlighted with the HDR-Fwd (forward) primer annealing outside the left homology arm. Rev, reverse.

(E) HDR frequency in HEK293T cells analyzed 96 hr after transfection of 1 μg pX330 and 1 μg *MALAT1* repair donor plasmid.

(F) Absolute (abs.) rate of HDR at the *MALAT1* locus. All editing experiments were performed in biological replicates (n ≥ 3). Data indicate the mean ± SEM. **p < 0.01.

(G) Western blot showing differential expression of hCas9 variants under genome-editing conditions (co-expression of repair donor plasmid and sgMALAT1 from pX330 vectors (1 μg each; 72 hr) in two independent experiments. Exp, experiment.

NHEJ pathway and was shown to improve HDR up to 19-fold (Chu et al., 2015; Maruyama et al., 2015). Surprisingly, we observed only minor, non-significant increases of HDR-mediated genome editing at the *MALAT1* locus, using two different SCR7 concentrations (1 μM and 10 μM) in HEK293T cells (Figure S2). This finding, although preliminary, questions the potential of SCR7 as a broadly active HDR-enhancing agent and highlights the need for alternative small-molecule compounds and molecular tools that have a more robust impact on HDR.

DISCUSSION

In summary, our study introduces a protein-engineering approach to control the expression and, thus, the activity of hCas9 in a temporal manner, which differs conceptually from previously developed inducible systems (Davis et al., 2015; Dow et al., 2015; Polstein and Gersbach, 2015; Zetsche et al., 2015b). We demonstrate that hCas9 can be controlled by intracellular regulatory circuits. The direct coupling of its expression with cell-cycle kinetics allows for a more efficient integration of exogenous sequences into a specific genomic locus. Here, we note that this regulatory concept might also be applicable to other genome-engineering proteins (TALEN, ZFN) and could also enable transcriptional (Gilbert et al., 2014; Konermann et al., 2015; Zalatan et al., 2015) or epigenetic (Hilton et al., 2015; Kearns et al., 2015) regulation in a cell-cycle-dependent manner.

Although our protein-engineering strategy resulted in improved HDR rates, we recognize that the observed enhancement in our study is moderate compared to other recently published strategies (Chu et al., 2015; Lin et al., 2014; Maruyama et al., 2015). Moreover, our study is somewhat compounded by the rather low overall rates of HDR. Especially, the absolute HDR rates of 0.17%–0.59% in our *EGFP* rescue assay (Figure 3) are about 10-fold lower than the previously reported rates using a similar cell system (Mali et al., 2013b). One explanation might be the use of HEK293T cells that harbor different random genomic integration sites of the disrupted *EGFP* gene, which might influence *EGFP* restoration due to differential DNA accessibility and/or higher order chromatin states (Wu et al., 2014). Additionally, Mali et al. (2013b) used separate plasmids to drive the expression of sgRNAs and hCas9, whereas the bicistronic pX330 vector delivers the sgRNA and hCas9 together. These different delivery and transfection strategies will ultimately lead to different molecular stoichiometries that might influence gene-editing efficiencies. Importantly, the observed HDR rates (about 9.7%–13.8%) at the endogenous *MALAT1* locus (Figure 4) are well within the range of observed recombination rates after plasmid-based delivery of hCas9 (Mali et al., 2013b; Pinder et al., 2015). These rates could be further increased to 12.7%–16.2% by transient G2/M arrest (Figure 5). In contrast, Lin et al. (2014) achieved absolute HDR rates as high as 38% upon sgRNA-Cas9 RNP complex transfection combined with nocodazole arrest in HEK293T cells, although these rates also varied between different gene loci and were largely dependent on the molecular stoichiometries.

Hence, testing various amounts of the hCas9-hGem(1/110) construct, using different guide RNAs and multiple genomic loci in diverse cellular systems, will reveal the full potential of this genome-engineering tool in the future.

Moreover, combination of hCas9-hGem(1/110) with complementary strategies has the potential to further improve HDR. For example, overexpression of Rad51 stimulates spontaneous homologous recombination (HR), break-induced intrachromosomal HR, and gene targeting by 2- to 7-fold (Arnaudeau et al., 1999; Lambert and Lopez, 2000; Xia et al., 1997; Yáñez and Porter, 1999), and co-expression of Rad51 or other HR proteins (Vasquez et al., 2001) with hCas9-hGem(1/110) might be beneficial. Alternatively, the Rad51-activating small-molecule RS-1 (Jayathilaka et al., 2008) was recently shown to enhance Cas9-based precise genome editing 3- to 6-fold (Pinder et al., 2015). However, the RS-1 effect range was, again, largely dependent on the molecular ratios and drug concentrations. Under optimized transfection conditions, HDR was enhanced by about 1.3-fold. Interestingly, treatment of cells with L755507, a recently discovered HDR stimulatory small molecule (Yu et al., 2015), had no significant effect by itself but partially synergized in combination with RS-1 and increased HDR ~1.8-fold (Pinder et al., 2015). It will be interesting to combine these compounds with the cell-cycle-tailored hCas9-hGem(1/110) variant introduced in this study.

Small-molecule-mediated inhibition of the NHEJ pathway represents a complementary approach, and DNA Ligase IV (SCR7) as well as DNA-PK (NU7441, KU-0060648) inhibitors had been combined with hCas9 and yielded higher HDR rates than hCas9 alone (Chu et al., 2015; Maruyama et al., 2015; Robert et al., 2015). SCR7 was reported to increase HDR up to 19-fold in human cell lines at a concentration of 1 μM (Maruyama et al., 2015). However, closer examination of the original data indicates that the improvement can be as low as 1.8-fold (Maruyama et al., 2015). Our own data (Figure S2), as well as those of others (Pinder et al., 2015; Robert et al., 2015), indicate that the SCR7 effect might strongly vary between different experimental systems. Thus, it will be important to understand these highly variable outcomes of the diverse molecules described earlier to identify potent small molecules that can broadly enhance HDR on a global rather than locus-specific or cell-type-restricted level.

Importantly, our regulatory concept, introduced here, takes advantage of cell-autonomous pathways to enable fluctuation of hCas9 protein levels coupled to cell-cycle dynamics. This resulted in higher site-specific integration events without sophisticated manipulation of cells by small molecules or additional gene-targeting reagents. Future methodological developments may enable high-resolution expression of hCas9 and alternative genome-engineering proteins such as Cpf1 (Zetsche et al., 2015a) by combining cell-cycle phase-specific transcriptional and post-translational regulatory elements. This might not only enhance HDR efficiencies even further but may also contribute to a better understanding of DNA repair pathways due to spatio-temporal control of DNA damage induction.

EXPERIMENTAL PROCEDURES

Cell Culture, Transfections, and Treatments

HEK293T cells (CRL 3216, ATCC), the HEK293T-derivative reporter line EGIP 293T (System Biosciences), and A549 lung cancer cells (CCL 185, ATCC) were cultured in DMEM supplemented with 10% fetal bovine serum (FBS), 2 mM

L-glutamine, 100 U/ml penicillin, and 100 mg/ml streptomycin. The cells were cultured at 37°C in a humidified chamber with 5% CO_2 and passaged 1:10 (A549) or 1:20 (HEK293T) twice a week. Presence of mycoplasma was routinely tested.

24 hr prior to transfection, 100,000 cells were plated in six-well plates. Transfection of indicated amounts of pX330 plasmids encoding respective sgRNAs and hCas9 variants was done using Lipofectamine 2000 (Life Technologies). All transfections were performed in technical triplicates, and fresh medium (with or without SCR7; S7742, Selleckchem) was added 7–9 hr after transfection. Cells treated with SCR7 (1–10 μM) were grown for additional 96 hr and subjected to HDR analysis. Synchronization of cells in G2/M was achieved by nocodazole treatment (S2775, Selleckchem; 200 ng/ml) for 20–22 hr.

CRISPR-Cas9 sgRNA Design and Plasmid Construction

The hCas9 expression plasmid (pX330) (Cong et al., 2013; Ran et al., 2013) was acquired from Addgene (plasmid #42230). To generate the hCas9-hGem(1/110) fusion, the pX330 plasmid was digested with FseI and EcoRI. The following DNA oligonucleotides were phosphorylated, annealed, and ligated with the digested vector to introduce restriction sites for BamHI, HindIII, and XhoI: MCS_F: CCAGGCAAAAAAGAAAAAGGGATCCAAGCTTCTCGAGG, MCS_R: AATTCCTCGAGAAGCTTGGATCCCTTTTTCTTTTTTGCCTGGCCGG. The N-terminal part of human Geminin (nt 208–537, NM_015895.4) encoding amino acid residues 1–110 was synthesized by GENEWIZ and inserted into the modified pX330 plasmid via HindIII and XhoI. Relevant sequence information of the pX330-U6-Chimeric_BB-CBh-hSpCas9-hGem(1/110) plasmid can be found in Figure 1C. The plasmid is available through Addgene (plasmid #71707).

The design of sgRNAs was based on recommendations from the Zhang laboratory website (http://crispr.mit.edu/). Cloning of sgRNAs into the pX330-hCas9 plasmid or pX330-hCas9-hGem(1/110) plasmid was done as described by Ran et al. (2013). The following DNA oligonucleotides for sgRNA cloning were ordered from Sigma-Aldrich:

sgAAVS1_sense: 5′-CACCGGGGCCACTAGGGACAGGAT-3′, sgAAVS1_antisense: 5′- AAACATCCTGTCCCTAGTGGCCCC-3′; sgMALAT1_sense: 5′-CACCGTACGCCTCGCCCGAGCTGTG-3′, sgMALAT1-antisense: 5′- AAACCACAGCTCGGGCGAGGCGTAC-3′.

MALAT1 Repair Donor Plasmid Construction

Left (787 bp) and right (801 bp) homology arms were amplified as described previously (Gutschner et al., 2011) and inserted into a modified pCRII-TOPO-TA dual promoter vector (Life Technologies). A multiple cloning site containing BamHI, XhoI, and NotI restriction sites separates the homology arms (see Figure 4D).

RNA Isolation and Real-Time qPCR

Cells were lyzed with TRIzol reagent (Life Technologies), and DNA-free RNA was isolated using the Direct-zol RNA MiniPrep Kit (Zymo Research) according to manufacturer's recommendations. For cDNA synthesis, 1 μg total RNA was reverse transcribed using random primers and the SuperScript III First-Strand Synthesis system (Life Technologies). Gene expression was measured on a Stratagene Mx3005P qPCR system (Agilent Technologies) using SYBR GreenER qPCR SuperMix (Life Technologies). ACTB was used as a reference gene in all real-time qPCR analyses. The following primer pairs were used: ACTB_F: 5′-TCAAGATCATTGCTCCTCCTGAG-3′, ACTB_R: 5′-ACATCTGCTGGAAGGTGGACA-3′; Cas9_F: 5′-CCGAAGAGGTCGTGAAGAAG-3′, Cas9_R: 5′-GCCTTATCCAGTTCGCTCAG-3′.

Immunoblot

Protein expression was analyzed as described previously (Gutschner et al., 2014). Anti-FLAG antibody (clone M2) was purchased from Sigma-Aldrich. Anti-Geminin antibody (#5165) was from Cell Signaling Technology. Anti-β-Actin antibody (clone AC-74) was from Sigma-Aldrich, and anti-Vinculin antibody (clone V284) was from EMD Millipore. Secondary HRP (horseradish peroxidase)-linked anti-mouse and anti-rabbit antibodies were purchased from Cell Signaling Technology. ImageJ software (http://imagej.nih.gov/ij/) was used for quantitative protein expression analysis.

Live-Cell Sorting

Prior to sorting, cells were incubated for 1 hr in medium containing Hoechst 33342 dye (5 μg/ml; Life Technologies). Cells were washed with PBS, harvested with Trypsin, spun down at 500 × g for 5 min, and re-suspended in 1 ml complete medium containing Hoechst 33342 (5 μg/ml). Cells were sorted according to their DNA content using an Influx Cell Sorter (Becton Dickinson). Approximately 10^6 cells were collected per G0/G1 and S/G2/M phase.

Isolation of Genomic DNA and PCR Amplification of *MALAT1* Target Region

Genomic DNA was isolated using the DNeasy Blood & Tissue Kit (QIAGEN).

A 393-nt region of *MALAT1*, containing the target site, was amplified using the following primer pair: MALAT1_SURV_F: 5′-TTGCAGCTCAAATCTTTCCA-3′, MALAT1_SURV_R: 5′- CGTTAAAAACTTAACGCTAAGCAA-3′. The resulting PCR product was used in subsequent SURVEYOR cleavage assays (discussed in the following text). An ~1,200-bp region of *MALAT1*, containing the target site and upstream sequences not included in the left homology arm of the *MALAT1* repair donor plasmid, was amplified using the following primer set: MALAT1_HDR_F: 5′- ACCTAACCAGG CATAACACAGAAT-3′, MALAT1_HDR_R: 5′- TCTTTTCCTTCCTCATGCTAC TCT-3′. The PCR reaction was performed using 200 ng of genomic DNA and Herculase II fusion polymerase with 5× reaction buffer (Agilent Technologies), according to the manufacturer's protocol. The thermocycler setting for SURVEYOR PCR consisted of one cycle of 95°C for 3 min; 31 cycles of 95°C for 20 s, 57°C for 30 s, and 72°C for 20 s; and one cycle of 72°C for 3 min. The settings for the HDR-PCR were: one cycle of 95°C for 3 min; 32 cycles of 95°C for 30 s, 60°C for 30 s, and 72°C for 45 s; and one cycle of 72°C for 3 min. PCR products were purified using the QIAquick PCR Purification Kit (QIAGEN).

SURVEYOR Nuclease Assay

The SURVEYOR Mutation Detection Kit for standard gel electrophoresis (Transgenomic) was used to assess the cleavage activity of sgMALAT1. In brief, 400 ng of SURVEYOR PCR product was incubated with Standard Taq Reaction buffer (New England Biolabs) at 95°C for 10 min in a metal heat block to allow DNA denaturation. Heteroduplex formation was induced by slow cooldown of the metal block after its removal from the heating block. Once the temperature of the metal block reached 25–30°C, an Enzyme-$MgCl_2$-Mix was added, according to the manufacturer's protocol, and the reaction was incubated at 42°C for 45 min. SURVEYOR nuclease digestion products (10 μl) were run on a 4%–20% gradient TBE (Tris-borate-EDTA) gel (Life Technologies). The gel was stained with SYBR Gold dye (1:10,000 diluted in fresh TBE; Life Technologies). The gel was imaged using the ChemiDoc XRS+ Imaging System with Image Lab 4.0 software (Bio-Rad) without allowing for oversaturation of DNA bands. Cleavage intensity was estimated by measuring the integrated intensity of the PCR amplicon and cleaved bands for each lane using ImageJ software (http://imagej.nih.gov/ij/). The fraction of cut PCR product was calculated using the following formula: $f_{cut} = (b + c)/(a + b + c)$, where a is the integrated intensity of the undigested PCR product, and b and c are the integrated intensities of each cleavage product. The following equation was used to estimate indel occurrence: indel (%) = $(1 - (1 - f_{cut})1/2) \times 100$.

Analysis of HDR at the Endogenous *MALAT1* Locus

XhoI directly cleaves PCR products containing the newly integrated XhoI restriction sequence as the result of successful HDR. The XhoI digestion reaction consisted of 150 ng purified PCR product and 0.5 μl FastDigest XhoI enzyme (Thermo Fisher Scientific) in 1× FastDigest reaction buffer. After 1 hr incubation at 37°C, the reaction mixtures (10 μl) were mixed with 5× Novex Hi-Density TBE sample buffer (Life Technologies) and run on a 4%–20% gradient TBE gel (Life Technologies). Gel staining, image acquisition, and image analysis was done as described earlier (see SURVEYOR Nuclease Assay). The percentage of HDR was calculated using the following equation: $((b + c) / (a + b + c)) \times 100$, where a is the band intensity

of the undigested full-length HDR-PCR product, and *b* and *c* are the cleavage products.

Analysis of HDR in the EGFP Reporter Assay

The Cas9 SmartNuclease AAVS1 Positive Control Kit (Cat. #CAS605A-1; System Biosciences) was purchased to analyze and compare HDR by hCas9 and hCas9-hGem(1/110) in an unbiased and reliable manner. The kit comes with an enhanced green fluorescent inhibited protein (EGIP) reporter cell line (HEK293T), which contains a single copy of a non-functional *EGFP* gene. *EGFP* expression can be restored by HDR using an *EGFP* rescue donor plasmid (included in the kit). This requires targeting of a 53-bp AAVS1 sequence that had been integrated into *EGFP* together with a stop codon to inactivate its expression. The AAVS1 sgRNA (Mali et al., 2013b) was cloned into the respective pX330 plasmids containing hCas9 or hCas9-hGem(1/110). Indicated amounts of plasmids were transfected, and EGFP-positive and viable (propidium-iodide-negative) cells were detected after 72 hr using a Gallios Flow Cytometer (Beckman Coulter). FlowJo software v.10 was used for flow cytometry data analysis.

Statistical Analysis

Significance was assessed using two-tailed Student's t tests after determination of the variance equality using an F test.

SUPPLEMENTAL INFORMATION

Supplemental Information includes two figures and can be found with this article online at http://dx.doi.org/10.1016/j.celrep.2016.01.019.

AUTHOR CONTRIBUTIONS

Conceptualization: T.G.; methodology, T.G.; investigation, T.G., M.H., and G.G.; formal analysis, T.G.; visualization, T.G.; writing—original draft, T.G.; writing—review and editing, T.G., M.H., G.G., G.F.D., and L.C.; funding acquisition, T.G., G.F.D., and L.C.; supervision, T.G. and L.C.

ACKNOWLEDGMENTS

The authors would like to thank Guocan Wang for helpful discussions and Ian R. Watson for critical reading of the manuscript. We thank all members of the MD Anderson Flow Cytometry and Cellular Imaging Core Facility for excellent technical assistance. The core facility is funded by the National Cancer Institute (NCI) Cancer Center Support grant P30CA16672.

L.C. is a CPRIT Scholar in Cancer Research and is supported by a grant from the Cancer Prevention Research Institute of Texas (R1204). T.G. is an Odyssey Postdoctoral Fellow and his work is supported in part by the Odyssey Program at The University of Texas MD Anderson Cancer Center. M.H. is supported by a Research Fellowship of the Deutsche Forschungsgemeinschaft (DFG).

Received: August 27, 2015
Revised: November 8, 2015
Accepted: January 1, 2016
Published: February 4, 2016

REFERENCES

Arnaudeau, C., Helleday, T., and Jenssen, D. (1999). The RAD51 protein supports homologous recombination by an exchange mechanism in mammalian cells. J. Mol. Biol. *289*, 1231–1238.

Barrangou, R., Fremaux, C., Deveau, H., Richards, M., Boyaval, P., Moineau, S., Romero, D.A., and Horvath, P. (2007). CRISPR provides acquired resistance against viruses in prokaryotes. Science *315*, 1709–1712.

Bolotin, A., Quinquis, B., Sorokin, A., and Ehrlich, S.D. (2005). Clustered regularly interspaced short palindrome repeats (CRISPRs) have spacers of extrachromosomal origin. Microbiology *151*, 2551–2561.

Brouns, S.J., Jore, M.M., Lundgren, M., Westra, E.R., Slijkhuis, R.J., Snijders, A.P., Dickman, M.J., Makarova, K.S., Koonin, E.V., and van der Oost, J. (2008). Small CRISPR RNAs guide antiviral defense in prokaryotes. Science *321*, 960–964.

Choi, P.S., and Meyerson, M. (2014). Targeted genomic rearrangements using CRISPR/Cas technology. Nat. Commun. *5*, 3728.

Chu, V.T., Weber, T., Wefers, B., Wurst, W., Sander, S., Rajewsky, K., and Kühn, R. (2015). Increasing the efficiency of homology-directed repair for CRISPR-Cas9-induced precise gene editing in mammalian cells. Nat. Biotechnol. *33*, 543–548.

Cong, L., Ran, F.A., Cox, D., Lin, S., Barretto, R., Habib, N., Hsu, P.D., Wu, X., Jiang, W., Marraffini, L.A., and Zhang, F. (2013). Multiplex genome engineering using CRISPR/Cas systems. Science *339*, 819–823.

Davis, K.M., Pattanayak, V., Thompson, D.B., Zuris, J.A., and Liu, D.R. (2015). Small molecule-triggered Cas9 protein with improved genome-editing specificity. Nat. Chem. Biol. *11*, 316–318.

Deltcheva, E., Chylinski, K., Sharma, C.M., Gonzales, K., Chao, Y., Pirzada, Z.A., Eckert, M.R., Vogel, J., and Charpentier, E. (2011). CRISPR RNA maturation by trans-encoded small RNA and host factor RNase III. Nature *471*, 602–607.

Doudna, J.A., and Charpentier, E. (2014). Genome editing. The new frontier of genome engineering with CRISPR-Cas9. Science *346*, 1258096.

Dow, L.E., Fisher, J., O'Rourke, K.P., Muley, A., Kastenhuber, E.R., Livshits, G., Tschaharganeh, D.F., Socci, N.D., and Lowe, S.W. (2015). Inducible in vivo genome editing with CRISPR-Cas9. Nat. Biotechnol. *33*, 390–394.

Garneau, J.E., Dupuis, M.E., Villion, M., Romero, D.A., Barrangou, R., Boyaval, P., Fremaux, C., Horvath, P., Magadán, A.H., and Moineau, S. (2010). The CRISPR/Cas bacterial immune system cleaves bacteriophage and plasmid DNA. Nature *468*, 67–71.

Gasiunas, G., Barrangou, R., Horvath, P., and Siksnys, V. (2012). Cas9-crRNA ribonucleoprotein complex mediates specific DNA cleavage for adaptive immunity in bacteria. Proc. Natl. Acad. Sci. USA *109*, E2579–E2586.

Gilbert, L.A., Horlbeck, M.A., Adamson, B., Villalta, J.E., Chen, Y., Whitehead, E.H., Guimaraes, C., Panning, B., Ploegh, H.L., Bassik, M.C., et al. (2014). Genome-Scale CRISPR-Mediated Control of Gene Repression and Activation. Cell *159*, 647–661.

Gutschner, T., Baas, M., and Diederichs, S. (2011). Noncoding RNA gene silencing through genomic integration of RNA destabilizing elements using zinc finger nucleases. Genome Res. *21*, 1944–1954.

Gutschner, T., Hämmerle, M., and Diederichs, S. (2013a). MALAT1 – a paradigm for long noncoding RNA function in cancer. J. Mol. Med. (Berl) *91*, 791–801.

Gutschner, T., Hämmerle, M., Eissmann, M., Hsu, J., Kim, Y., Hung, G., Revenko, A., Arun, G., Stentrup, M., Gross, M., et al. (2013b). The noncoding RNA MALAT1 is a critical regulator of the metastasis phenotype of lung cancer cells. Cancer Res. *73*, 1180–1189.

Gutschner, T., Hammerle, M., Pazaitis, N., Bley, N., Fiskin, E., Uckelmann, H., Heim, A., Grobeta, M., Hofmann, N., Geffers, R., et al. (2014). Insulin-like growth factor 2 mRNA-binding protein 1 (IGF2BP1) is an important protumorigenic factor in hepatocellular carcinoma. Hepatology *59*, 1900–1911.

Haemmerle, M., and Gutschner, T. (2015). Long non-coding RNAs in cancer and development: where do we go from here? Int. J. Mol. Sci. *16*, 1395–1405.

Haft, D.H., Selengut, J., Mongodin, E.F., and Nelson, K.E. (2005). A guild of 45 CRISPR-associated (Cas) protein families and multiple CRISPR/Cas subtypes exist in prokaryotic genomes. PLoS Comput. Biol. *1*, e60.

Hale, C.R., Zhao, P., Olson, S., Duff, M.O., Graveley, B.R., Wells, L., Terns, R.M., and Terns, M.P. (2009). RNA-guided RNA cleavage by a CRISPR RNA-Cas protein complex. Cell *139*, 945–956.

Haurwitz, R.E., Jinek, M., Wiedenheft, B., Zhou, K., and Doudna, J.A. (2010). Sequence- and structure-specific RNA processing by a CRISPR endonuclease. Science *329*, 1355–1358.

Heyer, W.D., Ehmsen, K.T., and Liu, J. (2010). Regulation of homologous recombination in eukaryotes. Annu. Rev. Genet. *44*, 113–139.

Hilton, I.B., D'Ippolito, A.M., Vockley, C.M., Thakore, P.I., Crawford, G.E., Reddy, T.E., and Gersbach, C.A. (2015). Epigenome editing by a CRISPR-Cas9-based acetyltransferase activates genes from promoters and enhancers. Nat Biotechnol. *33*, 510–517.

Hsu, P.D., Lander, E.S., and Zhang, F. (2014). Development and applications of CRISPR-Cas9 for genome engineering. Cell *157*, 1262–1278.

Ishino, Y., Shinagawa, H., Makino, K., Amemura, M., and Nakata, A. (1987). Nucleotide sequence of the iap gene, responsible for alkaline phosphatase isozyme conversion in Escherichia coli, and identification of the gene product. J. Bacteriol. *169*, 5429–5433.

Jayathilaka, K., Sheridan, S.D., Bold, T.D., Bochenska, K., Logan, H.L., Weichselbaum, R.R., Bishop, D.K., and Connell, P.P. (2008). A chemical compound that stimulates the human homologous recombination protein RAD51. Proc. Natl. Acad. Sci. USA *105*, 15848–15853.

Jinek, M., Chylinski, K., Fonfara, I., Hauer, M., Doudna, J.A., and Charpentier, E. (2012). A programmable dual-RNA-guided DNA endonuclease in adaptive bacterial immunity. Science *337*, 816–821.

Jinek, M., East, A., Cheng, A., Lin, S., Ma, E., and Doudna, J. (2013). RNA-programmed genome editing in human cells. eLife *2*, e00471.

Kearns, N.A., Pham, H., Tabak, B., Genga, R.M., Silverstein, N.J., Garber, M., and Maehr, R. (2015). Functional annotation of native enhancers with a Cas9-histone demethylase fusion. Nat. Methods *12*, 401–403.

Konermann, S., Brigham, M.D., Trevino, A.E., Joung, J., Abudayyeh, O.O., Barcena, C., Hsu, P.D., Habib, N., Gootenberg, J.S., Nishimasu, H., et al. (2015). Genome-scale transcriptional activation by an engineered CRISPR-Cas9 complex. Nature *517*, 583–588.

Lambert, S., and Lopez, B.S. (2000). Characterization of mammalian RAD51 double strand break repair using non-lethal dominant-negative forms. EMBO J. *19*, 3090–3099.

Lin, S., Staahl, B.T., Alla, R.K., and Doudna, J.A. (2014). Enhanced homology-directed human genome engineering by controlled timing of CRISPR/Cas9 delivery. eLife *3*, e04766.

Maddalo, D., Manchado, E., Concepcion, C.P., Bonetti, C., Vidigal, J.A., Han, Y.C., Ogrodowski, P., Crippa, A., Rekhtman, N., de Stanchina, E., et al. (2014). In vivo engineering of oncogenic chromosomal rearrangements with the CRISPR/Cas9 system. Nature *516*, 423–427.

Makarova, K.S., Grishin, N.V., Shabalina, S.A., Wolf, Y.I., and Koonin, E.V. (2006). A putative RNA-interference-based immune system in prokaryotes: computational analysis of the predicted enzymatic machinery, functional analogies with eukaryotic RNAi, and hypothetical mechanisms of action. Biol. Direct *1*, 7.

Makarova, K.S., Aravind, L., Wolf, Y.I., and Koonin, E.V. (2011a). Unification of Cas protein families and a simple scenario for the origin and evolution of CRISPR-Cas systems. Biol. Direct *6*, 38.

Makarova, K.S., Haft, D.H., Barrangou, R., Brouns, S.J., Charpentier, E., Horvath, P., Moineau, S., Mojica, F.J., Wolf, Y.I., Yakunin, A.F., et al. (2011b). Evolution and classification of the CRISPR-Cas systems. Nat. Rev. Microbiol. *9*, 467–477.

Mali, P., Esvelt, K.M., and Church, G.M. (2013a). Cas9 as a versatile tool for engineering biology. Nat. Methods *10*, 957–963.

Mali, P., Yang, L., Esvelt, K.M., Aach, J., Guell, M., DiCarlo, J.E., Norville, J.E., and Church, G.M. (2013b). RNA-guided human genome engineering via Cas9. Science *339*, 823–826.

Marraffini, L.A., and Sontheimer, E.J. (2008). CRISPR interference limits horizontal gene transfer in staphylococci by targeting DNA. Science *322*, 1843–1845.

Maruyama, T., Dougan, S.K., Truttmann, M.C., Bilate, A.M., Ingram, J.R., and Ploegh, H.L. (2015). Increasing the efficiency of precise genome editing with CRISPR-Cas9 by inhibition of nonhomologous end joining. Nat. Biotechnol. *33*, 538–542.

Mojica, F.J., Díez-Villaseñor, C., Soria, E., and Juez, G. (2000). Biological significance of a family of regularly spaced repeats in the genomes of Archaea, Bacteria and mitochondria. Mol. Microbiol. *36*, 244–246.

Mojica, F.J., Díez-Villaseñor, C., García-Martínez, J., and Soria, E. (2005). Intervening sequences of regularly spaced prokaryotic repeats derive from foreign genetic elements. J. Mol. Evol. *60*, 174–182.

Pinder, J., Salsman, J., and Dellaire, G. (2015). Nuclear domain 'knock-in' screen for the evaluation and identification of small molecule enhancers of CRISPR-based genome editing. Nucleic Acids Res. *43*, 9379–9392.

Platt, R.J., Chen, S., Zhou, Y., Yim, M.J., Swiech, L., Kempton, H.R., Dahlman, J.E., Parnas, O., Eisenhaure, T.M., Jovanovic, M., et al. (2014). CRISPR-Cas9 knockin mice for genome editing and cancer modeling. Cell *159*, 440–455.

Polstein, L.R., and Gersbach, C.A. (2015). A light-inducible CRISPR-Cas9 system for control of endogenous gene activation. Nat. Chem. Biol. *11*, 198–200.

Pourcel, C., Salvignol, G., and Vergnaud, G. (2005). CRISPR elements in Yersinia pestis acquire new repeats by preferential uptake of bacteriophage DNA, and provide additional tools for evolutionary studies. Microbiology *151*, 653–663.

Ran, F.A., Hsu, P.D., Wright, J., Agarwala, V., Scott, D.A., and Zhang, F. (2013). Genome engineering using the CRISPR-Cas9 system. Nat. Protoc. *8*, 2281–2308.

Robert, F., Barbeau, M., Éthier, S., Dostie, J., and Pelletier, J. (2015). Pharmacological inhibition of DNA-PK stimulates Cas9-mediated genome editing. Genome Med. *7*, 93.

Sakaue-Sawano, A., Kurokawa, H., Morimura, T., Hanyu, A., Hama, H., Osawa, H., Kashiwagi, S., Fukami, K., Miyata, T., Miyoshi, H., et al. (2008). Visualizing spatiotemporal dynamics of multicellular cell-cycle progression. Cell *132*, 487–498.

Sánchez-Rivera, F.J., Papagiannakopoulos, T., Romero, R., Tammela, T., Bauer, M.R., Bhutkar, A., Joshi, N.S., Subbaraj, L., Bronson, R.T., Xue, W., and Jacks, T. (2014). Rapid modelling of cooperating genetic events in cancer through somatic genome editing. Nature *516*, 428–431.

Sander, J.D., and Joung, J.K. (2014). CRISPR-Cas systems for editing, regulating and targeting genomes. Nat. Biotechnol. *32*, 347–355.

Schwank, G., Koo, B.K., Sasselli, V., Dekkers, J.F., Heo, I., Demircan, T., Sasaki, N., Boymans, S., Cuppen, E., van der Ent, C.K., et al. (2013). Functional repair of CFTR by CRISPR/Cas9 in intestinal stem cell organoids of cystic fibrosis patients. Cell Stem Cell *13*, 653–658.

Shalem, O., Sanjana, N.E., Hartenian, E., Shi, X., Scott, D.A., Mikkelsen, T.S., Heckl, D., Ebert, B.L., Root, D.E., Doench, J.G., and Zhang, F. (2014). Genome-scale CRISPR-Cas9 knockout screening in human cells. Science *343*, 84–87.

Shrivastav, M., De Haro, L.P., and Nickoloff, J.A. (2008). Regulation of DNA double-strand break repair pathway choice. Cell Res. *18*, 134–147.

Srivastava, M., Nambiar, M., Sharma, S., Karki, S.S., Goldsmith, G., Hegde, M., Kumar, S., Pandey, M., Singh, R.K., Ray, P., et al. (2012). An inhibitor of nonhomologous end-joining abrogates double-strand break repair and impedes cancer progression. Cell *151*, 1474–1487.

Vasquez, K.M., Marburger, K., Intody, Z., and Wilson, J.H. (2001). Manipulating the mammalian genome by homologous recombination. Proc. Natl. Acad. Sci. USA *98*, 8403–8410.

Wang, T., Wei, J.J., Sabatini, D.M., and Lander, E.S. (2014). Genetic screens in human cells using the CRISPR-Cas9 system. Science *343*, 80–84.

Wang, T., Birsoy, K., Hughes, N.W., Krupczak, K.M., Post, Y., Wei, J.J., Lander, E.S., and Sabatini, D.M. (2015). Identification and characterization of essential genes in the human genome. Science *350*, 1096–1101.

Wu, X., Scott, D.A., Kriz, A.J., Chiu, A.C., Hsu, P.D., Dadon, D.B., Cheng, A.W., Trevino, A.E., Konermann, S., Chen, S., et al. (2014). Genome-wide binding of the CRISPR endonuclease Cas9 in mammalian cells. Nat. Biotechnol. *32*, 670–676.

Xia, S.J., Shammas, M.A., and Shmookler Reis, R.J. (1997). Elevated recombination in immortal human cells is mediated by HsRAD51 recombinase. Mol. Cell. Biol. *17*, 7151–7158.

Xue, W., Chen, S., Yin, H., Tammela, T., Papagiannakopoulos, T., Joshi, N.S., Cai, W., Yang, G., Bronson, R., Crowley, D.G., et al. (2014). CRISPR-mediated direct mutation of cancer genes in the mouse liver. Nature *514*, 380–384.

Yáñez, R.J., and Porter, A.C. (1999). Gene targeting is enhanced in human cells overexpressing hRAD51. Gene Ther. *6*, 1282–1290.

Yu, C., Liu, Y., Ma, T., Liu, K., Xu, S., Zhang, Y., Liu, H., La Russa, M., Xie, M., Ding, S., and Qi, L.S. (2015). Small molecules enhance CRISPR genome editing in pluripotent stem cells. Cell Stem Cell *16*, 142–147.

Zalatan, J.G., Lee, M.E., Almeida, R., Gilbert, L.A., Whitehead, E.H., La Russa, M., Tsai, J.C., Weissman, J.S., Dueber, J.E., Qi, L.S., and Lim, W.A. (2015). Engineering complex synthetic transcriptional programs with CRISPR RNA scaffolds. Cell *160*, 339–350.

Zetsche, B., Gootenberg, J.S., Abudayyeh, O.O., Slaymaker, I.M., Makarova, K.S., Essletzbichler, P., Volz, S.E., Joung, J., van der Oost, J., Regev, A., et al. (2015a). Cpf1 Is a Single RNA-Guided Endonuclease of a Class 2 CRISPR-Cas System. Cell *163*, 759–771.

Zetsche, B., Volz, S.E., and Zhang, F. (2015b). A split-Cas9 architecture for inducible genome editing and transcription modulation. Nat. Biotechnol. *33*, 139–142.

Zhou, Y., Zhu, S., Cai, C., Yuan, P., Li, C., Huang, Y., and Wei, W. (2014). High-throughput screening of a CRISPR/Cas9 library for functional genomics in human cells. Nature *509*, 487–491.